

# Complete experimental characterization of stimulated Brillouin scattering in photonic crystal fiber

J.-C. Beugnot,<sup>1</sup> T. Sylvestre<sup>1</sup>, D. Alasia,<sup>1</sup> H. Maillotte,<sup>1</sup> V. Laude<sup>2</sup>,  
A. Monteville,<sup>3</sup> L. Provino,<sup>3</sup> N. Traynor,<sup>3</sup>  
S. Foaeng Mafang,<sup>4</sup> and L. Thévenaz<sup>4</sup>

<sup>1</sup>Département d'Optique P.M. Duffieux, Institut FEMTO-ST, Centre National de la Recherche Scientifique UMR 6174, Université de Franche-Comté, 25030 Besançon, France

<sup>2</sup>Département LPMO, Institut FEMTO-ST, Centre National de la Recherche Scientifique UMR 6174, Université de Franche-Comté, 25044 Besançon, France

<sup>3</sup>PERFOS, 11 rue de Broglie, 22300 Lannion, France

<sup>4</sup>Nanophotonics and Metrology Laboratory, École Polytechnique Fédérale de Lausanne, CH-1015, Lausanne, Switzerland.

[thibaut.sylvestre@univ-fcomte.fr](mailto:thibaut.sylvestre@univ-fcomte.fr)

**Abstract:** We provide a complete experimental characterization of stimulated Brillouin scattering in a 160 m long solid-core photonic crystal fiber, including threshold and spectrum measurements as well as position-resolved mapping of the Brillouin frequency shift. In particular, a three-fold increase of the Brillouin threshold power is observed, in excellent agreement with the spectrally-broadened Brillouin gain spectrum. Distributed measurements additionally reveal that the rise of the Brillouin threshold results from the broadband nature of the gain spectrum all along the fiber and is strongly influenced by strain. Our experiments confirm that these unique fibers can be exploited for the passive control or the suppression of Brillouin scattering.

© 2007 Optical Society of America

**OCIS codes:** (060.4005) Microstructured fibers; (060.2300) Fiber measurements; (060.4370) Nonlinear optics, fibers; (290.5830) Scattering, Brillouin

---

## References and links

1. P. St. J. Russell, "Photonic-crystal fibers," *J. Lightwave Technol.* **24**, 4729-4749 (2006).
2. V. Laude, A. Khelif, S. Benchabane, M. Wilm, T. Sylvestre, B. Kibler, A. Mussot, J. M. Dudley and H. Maillotte, "Phononic band-gap guidance of acoustic modes in photonic crystal fibers," *Phys. Rev. B* **71**, 045107 (2005).
3. P. Dainese, P. St. J. Russell, G. S. Wiederhecker, N. Joly, H. L. Fragnito, V. Laude, and A. Khelif, "Raman-like light scattering from acoustic phonons in photonic crystal fiber," *Opt. Express* **14**, 4141 (2006).
4. J.C. Beugnot, T. Sylvestre, H. Maillotte, G. Mélin, and V. Laude, "Guided acoustic wave Brillouin scattering in photonic crystal fibers," *Opt. Lett.* **2**, 17-19 (2007).
5. D. Elser, U. L. Andersen, A. Korn, O. Glckl, S. Lorenz, Ch. Marquardt, and G. Leuchs, "Reduction of guided acoustic wave Brillouin scattering in photonic crystal fibers," *Phys. Rev. Lett.* **97**, 133901 (2006).
6. P. Dainese, P. St. J. Russell, N. Joly, J.C. Knight, G.S. Wiederhecker, H.L. Fragnito, V. Laude and A. Khelif, "Stimulated Brillouin scattering from multi-GHz-guided acoustic phonons in nanostructured photonic crystal fibers," *Nature Physics* **2**, 388-392 (2005).
7. K. Furusawa, Z. Yusoff, F. Poletti, T.M. Monro, N.G.R. Broderick and D.J. Richardson, "Brillouin characterization of holey optical fibres," *Opt. Lett.* **17**, 2541-2543 (2006).
8. J. Toulouse, R. Pattnaik and J. McElhenny, "Stimulated Brillouin Scattering in Small Core Photonic Crystal Fibers (PCF)," in *Conf. on Lasers & Electro-Optics (Optical Society of America, Baltimore, 2007)* paper CThH7.

9. V.I. Kovalev and R.G. Harisson, "Waveguide-induced inhomogeneous spectral broadening of stimulated Brillouin scattering in optical fiber," *Opt. Lett.* **27**, 2022–2024 (2002).
  10. M. Gonzalez-Herraez and L. Thevenaz, "Simultaneous position-resolved mapping of chromatic dispersion and Brillouin shift along single-mode optical fibres," *Opt. Lett.* **4**, 1128–1130 (2004).
  11. R. Tkach, A. R. Chraplyvy and R. M. Derosier, "Spontaneous Brillouin scattering for single-mode optical fiber characterization," *Electron. Lett.* **22**, 1011–1012 (1986).
  12. P. Bayvel and P. M. Radmore "Solutions of the SBS equations in single mode optical fibers and implications for fiber transmission systems," *Electron. Lett.* **26**, 434–435 (1990).
  13. R. G. Smith, "Optical power handling capacity of low loss optical fibers as determined by stimulated Raman and Brillouin scattering," *Appl. Opt.* **11**, 2489–2494 (1972).
  14. G. P. Agrawal, *Nonlinear Fiber Optics*, 3rd Ed (Academic Press, Boston, 2001).
  15. M. O. van Devender and A.J. Boot, "Polarization properties of Stimulated Brillouin Scattering in Single Mode Fibers," *J. Lightwave Technol.* **12**, 585–590 (1994).
  16. W. Zhang, Y. Wang, Y. Pi, Y. Huang, and J. Peng, "Influence of pump wavelength and environment temperature on the dual-peaked Brillouin property of a small-core microstructure fiber," *Opt. Lett.* **32**, 2303–2305 (2007).
- 

## 1. Introduction

Photonic crystal fibers (PCFs) with a periodic air-hole microstructure exhibit unique and remarkable guiding and anti-guiding properties not only for optical waves but also for acoustic waves [1, 2]. In particular, the periodic wavelength-scale microstructure surrounding the PCF's core significantly impacts the transverse distribution of acoustic phonons, leading to new characteristics for both forward and backward stimulated Brillouin scattering (SBS) with respect to conventional all-silica fibers. For instance, recent observations have shown that forward Brillouin scattering in PCF is substantially enhanced at the GHz level, only for the fundamental acoustic phonon guided by the air-hole microstructure, while most of the other guided acoustic modes in the MHz range are quenched [3, 4, 5]. In addition, several recent papers have reported that the threshold power for backward SBS in small-core PCFs increases significantly [6, 7, 8]. As an example, in Ref. [6], an unexpected fivefold increase in SBS threshold has been measured in a ultra-small core PCF with a corresponding multi-peaked SBS spectrum. The multi-peaked structure was attributed to several families of guided acoustic modes, each with different proportions of longitudinal and shear strain, strongly localized to the core. In Ref. [7], the threshold growth was rather attributed to structural variations along the fiber and it was suggested that a controlled variation of the structural parameters can be used to design Brillouin-suppressed PCFs. However, it is significant that the origin of the rise in the SBS threshold has not been fully explored and clearly understood yet. The microstructure of PCFs could also lead to waveguide-induced inhomogeneous broadening of SBS gain, as recently evidenced in conventional single-mode fibers [9].

The aim of the present work is to clearly identify and understand the broadband and multi-mode nature of SBS spectra in PCFs as resulting from either the structural irregularities of the PCF or the PCF's microstructure that allows for the simultaneous generation and propagation of a fan of acoustic modes. For that purpose, we provide a complete experimental characterization of SBS in a 160-m long photonic crystal fiber with an intermediate core size ( $5\mu\text{m}$ ). The first part of the manuscript presents measurements of Brillouin threshold power and spectrum using an heterodyne technique. We found that the SBS threshold increases threefold compared with a uniform all-silica fiber and that this is in quite good agreement with the Brillouin linewidth broadening by 80 MHz. Then, we present position-resolved mapping of the Brillouin frequency shift using Brillouin optical domain time analysis (BOTDA) [10]. The results of our measurements show a broad asymmetric SBS gain spectrum distributed all along the fiber and indicate that the structural variations of the PCF have actually little impact on the Brillouin frequency shift.

## 2. Brillouin threshold and spectrum measurements

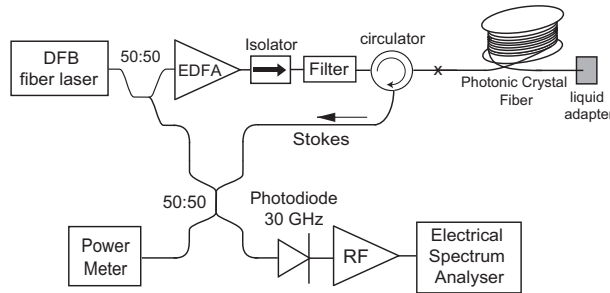


Fig. 1. Experimental setup for measuring Brillouin threshold and the gain spectra.

Figure 1 shows the first experimental setup for measuring the SBS threshold and the gain spectra. The experiment was performed using a distributed-feedback laser (DFB) emitting at a wavelength of 1549.74 nm (linewidth  $<45$  kHz). The laser output was split into two parts. The first portion was amplified by an EDFA and then passed through a 5-nm bandpass filter and an optical circulator. The PCF was connected to a standard single-mode fiber (SMF-28) via a high numerical-aperture (HNA) fiber by use of an Ericsson FSU-975 PM splicer and by using an home-made repeated discharge technique. A coupling efficiency of 80% was thereby achieved. To avoid feedback and Brillouin-induced lasing, we immersed the output end of the PCF in an index matching liquid. SBS was measured versus the input power by using a conventional heterodyne detection in which the second portion of the laser output is mixed through a 3-dB coupler with the backscattered Stokes wave [11]. The PCF was provided by PERFOS (Type HF-148M1A) and consists of a triangular lattice with a core and hole diameter equal to  $4.4 \mu\text{m}$  and  $1.4 \mu\text{m}$  respectively (see the cross-section in the inset of Fig. 2(a)). It has an effective area of  $12 \mu\text{m}^2$  at 1550 nm and a transmission loss of less than 2.7 dB/km.

The transmitted and backscattered powers as a function of the input pump power are illustrated in Fig 2.(a). We define the Brillouin threshold power as the input power for which the backscattered power reaches 1% of the input pump power [12] and is equal to 23.5 dBm in Fig 2(a). Applying the standard model as in Refs. [13, 14, 15] to an all-silica fiber with the same nonlinear coefficient and effective mode area, the SBS threshold of our PCF can be es-

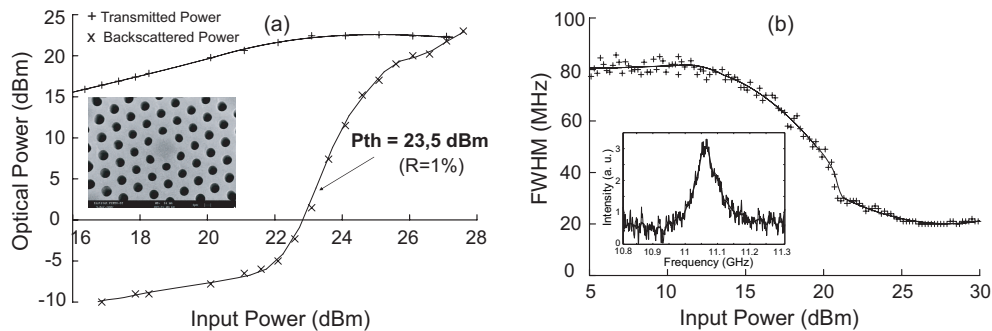


Fig. 2. (a) Measured transmitted and backscattered powers as a function of the input pump power. Inset, SEM image of PCF cross section. (b) Brillouin spectrum linewidth as a function of injected pump power. Inset, Brillouin spectrum below threshold (-15dB) using a heterodyne detection with 300 kHz of resolution, FWHM = 80MHz.

estimated to about 19 dBm, which is nearly three times less than the measured threshold power. Figure 2.(b) shows the Brillouin gain linewidth (FWHM) as a function of the input pump power. The inset depicts the gain spectrum below threshold (at -15dB) with a corresponding 80-MHz spectral width. Increasing the pump power leads to a narrowing of the SBS gain linewidth to 20 MHz. These values are nearly three times larger than the SBS spectrum dynamics for all-silica fibers [14] ( $\Delta\nu_B \simeq 25$  MHz), in very good agreement with the threefold increase in SBS threshold previously measured. Correspondingly, this means that the usual expression of SBS threshold for standard fibers remains valid for PCF if the spectrally-broadened SBS spectrum is carefully taken into account in the gain expression [13, 14].

### 3. Position-resolved Brillouin gain spectrum mapping

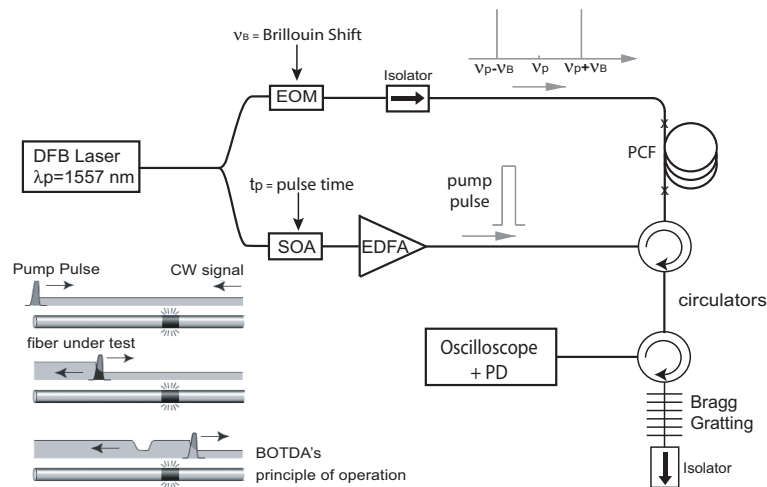


Fig. 3. Experimental setup for distributed SBS measurement in PCF. Bottom left : principle of operation of BOTDA technique.

Figure 3 is a sketch of the second experimental setup for mapping the SBS frequency shift. This distributed measurement is based on a recently-developed pump-probe technique called Brillouin optical time domain analysis (BOTDA) [10]. A CW DFB laser source at 1557 nm, similar to that of the previous setup, was split into pump and probe waves. The first portion (the pump) was then pulsed by gating a semiconductor optical amplifier (SOA) with an electrical pulse train, and the output pulses were amplified by an EDFA up to a few hundred mW. The pulses were launched into the PCF under test through an optical circulator in the counter-propagating direction to provide local Brillouin gain at the CW-probe signal. The probe was then intensity-modulated by an electro-optical modulator (EOM) to create two modulation frequencies at Brillouin Stokes ( $-\nu_B$ ) and anti-Stokes ( $\nu_B$ ), respectively, while suppressing the carrier by properly setting the DC voltage of the EOM. The amplified probe was measured using a photodiode (PD) and data were recorded using a digital oscilloscope synchronized with the Brillouin-pump pulse. By simply varying the frequency of the continuous probe wave relatively to the pump frequency, the Brillouin gain spectrum could then be fully retrieved at any location along the fiber and the Brillouin shift ( $\nu_B$ ) be unambiguously determined as a function of distance. This method offers several advantages such as no laser frequency drift dependence and no need for a tunable laser source [10]. Since the spatial resolution is given by the pulse duration, we performed two experiments with pulse durations of 20ns and 100ns, respectively.

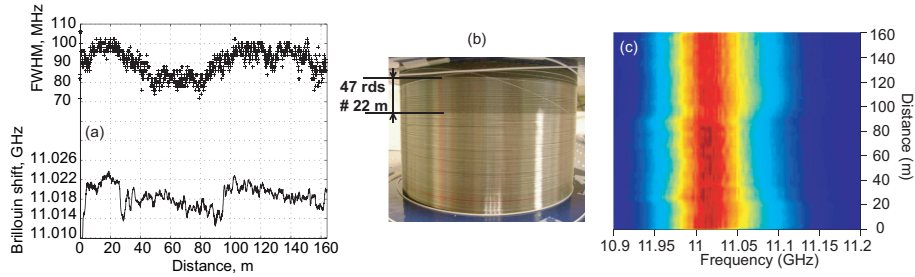


Fig. 4. (a) SBS gain width (FWHM, crosses) and frequency shift (solid line) versus distance with a spatial resolution of 2m. (b) fiber spool, (c) gain spectrum evolution.

Figures 4(a) and (c) show the distributed measurement of the SBS frequency shift and spectral width (FWHM), with a spatial resolution of 2 m. Figure 5 shows the same measurement but with a pump pulse width of 100 ns. This corresponds to a lower spatial resolution of 10-m but the Brillouin gain spectrum is more accurately detailed when compared to Fig. 4(c). First, it is clear from these measurements that longitudinal structural variations of the air-hole microstructure due to the drawing process has a stronger impact on the SBS frequency shift than in standard single-mode fiber (SMF) [7]. By examining both the short-scale and long-scale fluctuations, we assessed a SBS frequency drift with a corresponding maximum amplitude of about 10 MHz, which is ten times larger than routinely observed in SMF. This is significant but not enough to fully account for the total Brillouin linewidth broadening by 80 MHz.

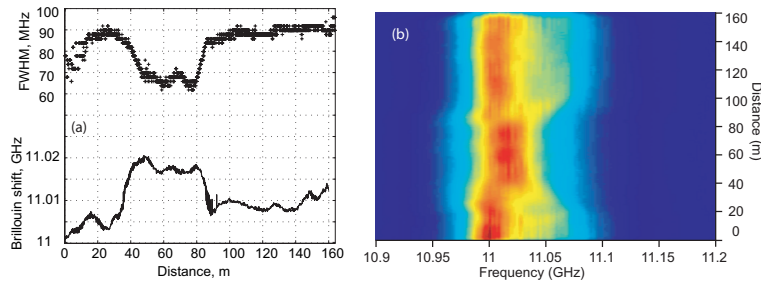


Fig. 5. (a) SBS gain width (FWHM, crosses) and frequency shift (solid line) versus distance with a spatial resolution of 10m. (b) evolution of SBS gain spectrum along the fiber.

In addition, we can observe in Figs. 4(c) and Fig. 5(a) a large frequency shift ( $\sim 30$  MHz) from 25 m until 90 m, with a corresponding reduction of the gain spectral width, from 90 MHz to about 65 MHz. Such an important frequency shift can be explained by considering the acoustic velocity,  $v_a$ , which is strain-dependent in optical fibers. Therefore the central frequency of the Brillouin spectrum  $\nu_B$  is expected to vary when the fiber is under stress. As we can see on the photograph of Fig. 4(b), the first portion of the PCF seems to be under stress as a result of winding by the subsequent portion of the fiber. The 22-m length of the first part corresponds in good agreement to the beginning of the SBS frequency shift shown in Figs 4 and 5. Actually, the gain spectrum shown in Fig. 5(b) reveals the co-existence of two strongly-coupled acoustic modes within the PCF core and frequency-shifted by more than 40 MHz. This can be viewed in detail in Fig. 6 that presents gain spectra at different lengths with a corresponding dual-peak structure, except at distances 45m, 70 m and 90m. This is a clear illustration of the stress applied during winding which modifies the acoustic modal distribution and suppresses the highest frequency acoustic modes.

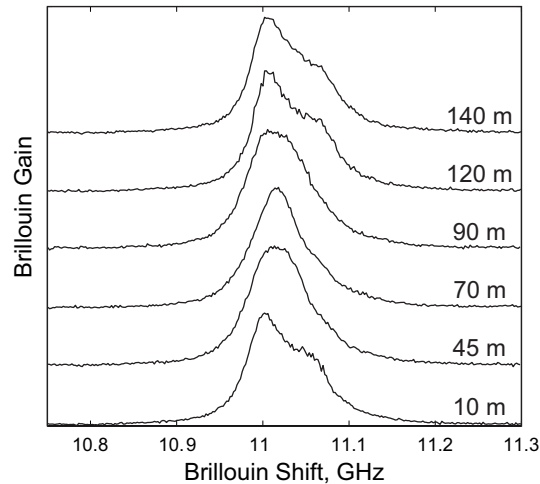


Fig. 6. Brillouin spectrum at different position along the fiber for a 100ns pulse. The entire sequence can be viewed as a movie attached to the manuscript (avi, 2290 kb).

We must stress that these two acoustic modes cannot be attributed to modal birefringence ( $\Delta n = 3 \times 10^{-5}$ ) since it would lead to a much smaller acoustic frequency shift between the low and fast birefringent axes equal to  $\Delta f = 2\Delta n \frac{v_a}{\lambda_p} = 0.23$  MHz. Consequently, we can rationally attribute this dual-peak broad SBS spectrum to the microstructure itself that fundamentally alters the Brillouin scattering process by its ability to enable the generation of two closely-spaced acoustic phonons. Note that a similar dual-peaked Brillouin property of a small-core PCF has recently been reported and shown to be strongly influenced by the pump wavelength and environment temperature [16]. In the same way, we can expect that the two Brillouin peaks can independently be controlled by applying stress along the fiber. We can also deduce from Fig. 6 that, for increasing the SBS threshold, it is necessary to have several acoustic modes not far away (less than one mode linewidth), in which case they couple together.

#### 4. Conclusion

A position-resolved mapping of the Brillouin gain spectrum in a long photonic crystal fiber has been carried out for the first time. A threefold increase in the Brillouin threshold was also measured compared with a uniform all-silica fiber, as previously reported in other ultra small-core PCFs [1]. Our observations have shown that the significant reduction of SBS was in quite good agreement with the Brillouin linewidth broadening. This broadening cannot be attributed to the structural variation of the fiber but rather to the air-hole microstructure itself that allows for the guiding of several acoustic modes over a broader frequency range, with respect to conventional all-silica fiber. Moreover, distributed measurements demonstrated that some of these acoustic modes are very sensitive to stress applied along the fiber. Finally, our experimental work may help in designing future Brillouin-suppressed photonic crystal fibers and in the understanding of the complex light-sound interactions in microstructured materials.

#### Acknowledgments

This work has been supported by the European COST Action 299 and the European INTERREG-III project.